

EphrinB2 regulates osteogenic differentiation of periodontal ligament stem cells and alveolar bone defect regeneration in beagles

Journal of Tissue Engineering
Volume 10: 1–13
© The Author(s) 2019
Article reuse guidelines:
sagepub.com/journals-permissions
DOI: 10.1177/2041731419894361
journals.sagepub.com/home/tej



Penglai Wang^{1*}, Wen Wang^{1*}, Tengyu Geng¹, Yi Liu¹,
Shaoyue Zhu², Zongxiang Liu¹ and Changyong Yuan¹ 

Abstract

EphrinB2, a membrane protein regulating bone homeostasis, has been demonstrated to induce osteogenic gene expression in periodontal ligament fibroblasts. The aim of this study was to explore the effects of ephrinB2 on osteogenic differentiation of periodontal ligament stem cells and on alveolar bone regeneration *in vivo*. We assessed the osteogenic gene expression and osteogenic differentiation potential of ephrinB2-modified human and canine periodontal ligament stem cells, in which ephrinB2 expression was upregulated via lentiviral vector transduction. EphrinB2-modified canine periodontal ligament stem cells combined with PuraMatrix were delivered to critical-sized alveolar bone defects in beagles to evaluate bone regeneration. Results showed that ephrinB2 overexpression enhanced osteogenic gene transcription and mineral deposition in both human and canine periodontal ligament stem cells. Animal experiments confirmed that ephrinB2-modified canine periodontal ligament stem cells + PuraMatrix resulted in greater trabecular bone volume per tissue volume and trabecular thickness compared with other groups. Our study demonstrated that ephrinB2 promoted osteogenic differentiation of periodontal ligament stem cells and alveolar bone repair in beagles, highlighting its therapeutic potential for the treatment of alveolar bone damage.

Keywords

EphrinB2, osteogenesis, bone regeneration, PDLSCs

Date received: 11 October 2019; accepted: 18 November 2019

Introduction

In severe periodontitis, bacteria-induced inflammation causes destruction of the tooth supporting structure, which if left untreated will lead to tooth loss. Current conventional strategies aiming to eliminate pathogenic biofilms and control infection and inflammation, either nonsurgically or surgically, cannot regenerate functional periodontal tissues.^{1,2} Even using various regenerative procedures, such as bone grafting, guided tissue/bone regeneration, use of recombinant growth factors, and enamel matrix derivative applications,^{3,4} success in regenerating periodontium is limited and unpredictable. Therefore, development of novel tissue engineering strategies to completely regenerate the lost alveolar bone, periodontal ligament (PDL), and cementum is urgently required.

It has been shown that stem cell-based strategies achieve greater efficacy in periodontal regeneration.⁵ It

¹Affiliated Stomatological Hospital of Xuzhou Medical University, Xuzhou, China

²Faculty of Dentistry, The University of Hong Kong, Pokfulam, Hong Kong

*Penglai Wang and Wen Wang contributed equally to this work.

Corresponding authors:

Zongxiang Liu, Affiliated Stomatological Hospital of Xuzhou Medical University, No. 130 Huaihai West Road, Xuzhou 221000, Jiangsu, China.
Email: 408571191@qq.com

Changyong Yuan, Affiliated Stomatological Hospital of Xuzhou Medical University, No. 130 Huaihai West Road, Xuzhou 221000, Jiangsu, China.
Email: 24503692@qq.com



has been well validated that stem cells, including periodontal ligament stem cells (PDLSCs), bone marrow mesenchymal stem cells (BMSCs), and periosteal- and adipose-derived stem cells, induce periodontal regeneration in animal models.^{6,7} Compared with other mesenchymal stem cells, PDLSCs exhibit a marked ability to generate multiple tissue types *in vivo*, including Sharpey's fibers, alveolar bone, and cementum.^{8–10} However, many unresolved issues remain, such as washing out and low integration of transplanted cells, inflammatory reactions to toxic degradation products, and insufficient bone formation in cases of severe bone loss.

Regenerating the resorbed alveolar bone in severe periodontitis is a major challenge. Interaction between ephrinB2 and EphB4, expressed, respectively, in osteoclasts and osteoblasts, inhibits osteoclastic differentiation and enhances osteoblastic differentiation, thus maintaining bone homeostasis.¹¹ Recombinant ephrinB2-Fc could stimulate osteogenic differentiation of BMSCs and pre-osteoblastic cells via forward signaling, mediated by EphB2 or EphB4 receptor.^{12–14} EphrinB2/EphB4 signaling also plays an important role in mechanical forces regulating bone formation.^{15,16} Blockade of EphrinB2/EphB4 interaction in osteoblasts has been shown to inhibit osteogenic gene expression and mineralization, which suggests that osteoblastic ephrinB2 might act on its EphB4 receptor in a paracrine or autocrine manner.^{17,18}

Similarly, PDLSCs express ephrinB2 and its corresponding receptors, which could be regulated by mechanical forces and by lipopolysaccharide.^{16,19} EphrinB2-Fc can induce runt-related transcription factor 2 (RUNX2) and alkaline phosphatase (ALP) transcription in PDL fibroblasts,¹⁶ meaning it might be a potential regulator for stimulating osteogenic differentiation of PDLSCs. However, as a recombinant protein with a short half-life, ephrinB2-Fc can hardly maintain a stable biological effect. Therefore, overexpressing ephrinB2 in PDLSCs might provide a more viable means of enhancing osteogenic regeneration than applying exogenous ephrinB2-Fc. To test this hypothesis, we generated ephrinB2-modified human periodontal ligament stem cells (hPDLSCs) and canine periodontal ligament stem cells (cPDLSCs), and we further investigated their osteogenic potential *in vitro* and their alveolar bone regeneration capacities *in vivo*.

Materials and methods

Cell culture and characterization

Human PDLSCs were obtained from wisdom teeth extracted from volunteers aged 18–25 years, with their consent and approval from the Ethics Committee of Xuzhou Medical University (Xuzhou, China; No. 20161108). cPDLSCs were isolated from the freshly extracted anterior teeth of six beagles (male, 15 months old), which were obtained from the

Experimental Animal Center of Xuzhou Medical University. The Experimental Animal Ethics Committee of Xuzhou Medical University approved the usage of dogs as well as harvesting of their tissues (No. 20161108).

PDL tissues scraped from the middle-third root surfaces were digested in α -minimum essential medium (α -MEM; Gibco, Thermo Fisher Scientific, Beijing, China) containing 3 mg/mL collagenase type I (Gibco, Life Technologies, Grand Island, NY, USA) and 4 mg/mL dispase (Gibco Life Technologies) for 1 h at 37°C. Then, cells and the remaining tissues were cultured in α -MEM supplemented with 10% fetal bovine serum (FBS; Gibco, Rio de Janeiro, Brazil, South America), 100 U/mL penicillin, and 100 μ g/mL streptomycin (Vicmed, Xuzhou, Jiangsu, China). Cells between passages 2 and 6 were used for subsequent experiments.

To evaluate colony-forming properties, we seeded a single-cell suspension into six-well plates (200 cells/well) or 6 cm dishes (400 cells/dish). After 10 days, colonies were fixed with 4% (w/v) paraformaldehyde and stained with crystal violet.

To analyze mesenchymal stem cell markers, we incubated cells at passage 2 (2.5×10^5 cells/tube) at room temperature for 45 min with the following fluorescent-conjugated monoclonal antibodies: CD90 PerCP, CD73 FITC, CD45 APC, CD105 APC (BD Biosciences, San Jose, CA, USA), and STRO-1 PE (Santa Cruz Biotechnology, Dallas, TX, USA). Next, the cells were run through a flow cytometer (FACS Canto II; BD Biosciences).

To induce osteogenic differentiation, we cultured cells in α -MEM containing 10% FBS, 10 mmol/L β -glycerophosphate, 50 μ g/mL L-ascorbic acid phosphate, and 10 nmol/L dexamethasone. To induce adipogenic differentiation, we cultured cells in α -MEM containing 10% FBS, 1 μ mol/L dexamethasone, 1 μ g/mL insulin, and 0.5 mmol/L 3-isobutyl-1-methylxanthine. To induce neurogenic differentiation, we cultured cells in Neurobasal A medium (Gibco, Thermo Fisher Scientific) supplemented with 40 ng/mL basic fibroblast growth factor (bFGF; PeproTech, Inc., Rocky Hill, NJ, USA) and 20 ng/mL epidermal growth factor (EGF; PeproTech Inc.). After 4 weeks, Alizarin Red S staining, ALP staining, Oil Red O staining, and immunofluorescence staining for β III-tubulin were performed.

EphrinB2 gene transduction by lentivirus

Lentiviral particles for ephrinB2 (human, LPP-M0409-Lv233-400; dog, LPP-GS-Md02143-Lv201-400) and corresponding control lentiviral particles (human, LPP-EGFP-Lv233-100; dog, LPP-NEG-Lv201-100) were purchased from GeneCopoeia (Rockville, MD, USA). PDLSCs at passage 1 were seeded into six-well plates (2.5×10^5 cells/well) and infected with either 40 μ L lentiviral particles for ephrinB2 or 8 μ L control lentiviral particles in the presence of 4 μ g/mL polybrene (Vicmed) for

Table 1. Sequences of human and canine primers used in quantitative polymerase chain reaction.

Species	Gene	Primers
<i>Homo sapiens</i>	EphrinB2	Forward: 5'-TATGCAGAACTGCGATTTCCAA-3' Reverse: 5'-TGGGTATAGTACCAGTCCTTGTC-3'
	ALP	Forward: 5'-CCTCGTTGACACCTGGAAGAG-3' Reverse: 5'-TTCCGTGCGGTTCCAGA-3'
	RUNX2	Forward: 5'-TCTTAGAACAAATCTGCCCTTT-3' Reverse: 5'-TGCTTTGGTCTTGAAATCACA-3'
	BMP2	Forward: 5'-TTCCACCATGAAGAATCTTTGGA-3' Reverse: 5'-CCTGAAGCTCTGCTGAGGTGAT-3'
	COL1	Forward: 5'-GAGGGCCAAGACGAAGACATC-3' Reverse: 5'-CAGATCACGTCATCGCACAAAC-3'
	OCN	Forward: 5'-CTACCTGTATCAATGGCTGGG-3' Reverse: 5'-GGATTGAGCTCACACACCT-3'
	β -actin	Forward: 5'-ACGTTGCTATCCAGGCTGTG-3' Reverse: 5'-GGCCATCTCTTGCTCGAAGT-3'
<i>Canis familiaris</i>	ALP	Forward: 5'-GGTGAGTGACACGGACAAGAAGC-3' Reverse: 5'-GCCTGGTAGTTGTTGTGAGCGTAG-3'
	RUNX2	Forward: 5'-TACCACACCTACCTGCCACCAC-3' Reverse: 5'-GCGGAAGCATTCTGGAAGGAGAC-3'
	BMP2	Forward: 5'-TGAAGTCCACTAACCACGCCATTG-3' Reverse: 5'-TGTTGGTACACAGCACGCCTTG-3'
	COL1	Forward: 5'-GCCTGGTAGTTGTTGTGAGCGTAG-3' Reverse: 5'-CACCGTCATCTCCGTTCTTGCC-3'
	EphrinB2	Forward: 5'-TGCCAGACAAGAGCCATGAAGATC-3' Reverse: 5'-GGCGTCGTGTTGGATCATTATGC-3'
	EphB4	Forward: 5'-AGGAGCACCACAGCCAGACC-3' Reverse: 5'-AGCAATGACAATGACCACCAGGAC-3'
	β -actin	Forward: 5'-ATCACTATTGGCAACGAGCGGTTTC-3' Reverse: 5'-CAGCACTGTGTTGGCATAGAGGTC-3'

ALP: alkaline phosphatase; RUNX2: runt-related transcription factor 2; BMP2: bone morphogenetic protein 2; COL1: collagen type I; OCN: osteocalcin.

12 h. Stably transfected cells were selected by 1.5 μ g/mL puromycin (Vicmed). Gene transfer efficiency was assessed by green fluorescence expression and ephrinB2 messenger RNA (mRNA) and protein expression.

Cell proliferation assay

Cells were plated at 5000 cells per well into five 96-well plates, and cell numbers were assessed on days 0, 2, 4, 6, and 8 using a Cell Counting Kit-8 (CCK-8; Vicmed) according to the manufacturer's protocol. Briefly, cells were incubated in 100 μ L α -MEM containing 10 μ L CCK-8 for 1 h at 37°C, and then absorbance at 450 nm was measured. Each group had three replica wells, and the assay was repeated three times.

ALP and Alizarin Red S staining

After osteogenic induction, cells were fixed with 4% (w/v) paraformaldehyde and stained with nitro blue tetrazolium/5-bromo-4-chloro-3'-indolyphosphate (NBT/BCIP) substrate solution (Beyotime Institute of Biotechnology, Shanghai, China) for 1 h or 2% (w/v) Alizarin Red S

solution (pH 4.2) for 30 min. Staining intensity was quantified with Image J.

Quantitative polymerase chain reaction

Total RNA was isolated using TRIzol Reagent (Invitrogen, Carlsbad, CA, USA) and quantified by NanoDrop2000 spectrophotometer (Thermo Fisher Scientific, Wilmington, DE, USA). The purified RNA was reverse transcribed to cDNA using HiScript Q RT SuperMix for quantitative polymerase chain reaction (qPCR) (Vazyme Biotech Co., Ltd, Nanjing, Jiangsu, China) according to the manufacturer's protocol. The qPCR reaction mixture (20 μ L) contained 2 μ L cDNA, 100 nM forward and reverse primers, and 1 \times UltraSYBR Mixture (CWbio, Beijing, China). Primers are listed in Table 1. All qPCR assays were performed in an ABI 7500 sequence detection system (Applied Biosystems, Darmstadt, Germany) under the following conditions: 95°C for 10 min, 40 cycles at 95°C for 15 s and 60°C for 1 min, followed by melt curve analysis at 95°C for 15 s, 60°C for 1 min, 95°C for 15 s, and 60°C for 15 s. Values were normalized to β -actin using the comparative cycle threshold method ($\Delta\Delta$ CT).

Western blotting

Cells were lysed with radioimmunoprecipitation assay buffer (RIPA) buffer (Beyotime Institute of Biotechnology) and 1 mM phenylmethylsulfonyl fluoride (PMSF) (Beyotime Institute of Biotechnology). Forty micrograms of protein was separated by 10% sodium dodecyl sulfate polyacrylamide gel electrophoresis (SDS-PAGE) under reducing conditions and transferred onto nitrocellulose membranes (Pall Corp., Pensacola, FL, USA). Blocked in 5% (w/v) milk for 1 h, membranes were then incubated with the following primary antibodies overnight at 4°C: anti-ephrinB2 (1:2000; Abcam, Cambridge, UK), anti-phospho-ephrinB2 (Tyr324/329; 1:500; Cell Signaling Technology, Danvers, MA, USA), anti-EphB4 (1:200; Santa Cruz Biotechnology, Dallas, TX, USA), anti-phospho-EphB4 (1:1000; Signalway Antibody, College Park, MD, USA), and anti- β -actin (1:3000, Beyotime Institute of Biotechnology). Blots were then incubated with horseradish peroxidase-conjugated goat anti-rabbit or anti-mouse secondary antibodies (Proteintech, Wuhan, Hubei, China). Tanon4500 Immunodetection System (Tanon Science & Technology Co., Ltd., Shanghai, China) was used for visualization of blots. Quantification of the blots was performed using Image J.

Cell encapsulation within PuraMatrix

To transplant cPDLSCs into alveolar bone defects *in vivo*, 0.25% PuraMatrix (BD Biosciences, Bedford, MA, USA) was used as a scaffold. Equal volumes of 1% PuraMatrix and 20% sterile sucrose were mixed to generate 0.5% PuraMatrix in 10% sucrose. cPDLSCs transfected with ephrinB2 lentiviral particles (EfnB2-cPDLSCs) or control lentiviral particles (Vector-cPDLSCs) were trypsinized and resuspended in 10% sucrose at a density of 8×10^6 cells/mL. EfnB2-cPDLSCs/PuraMatrix or Vector-cPDLSCs/PuraMatrix constructs were prepared by mixing equal volumes of cells/sucrose and 0.5% PuraMatrix. The mixtures were transferred into 24-well plates (400 μ L/well), and then medium (500 μ L/well) was added. The medium was changed twice over a period of 1 h to equilibrate pH. The cells/PuraMatrix complexes were cultured with osteo-inductive supplements for 1 week before transplanted into defects.

Surgical procedures for animal experiments

The six dogs that provided the anterior teeth for isolation of cPDLSCs were used in the animal experiments. All experimental procedures were performed according to the Treatment of Experimental Animal Protocol of Xuzhou Medical University and were approved by the Experimental Animal Ethics Committee of Xuzhou Medical University (No. 20161108).

All surgical procedures were carried out with the dogs under general anesthesia induced by intravenous injection of propofol (2 mg/kg) and inhalation of isoflurane

(1.5%–2%) and O₂ (100%). Local infiltration anesthesia was induced by administering 4% articaine with 1:100,000 epinephrine at the surgical sites. Bilateral mandibular third premolars were split via furcation and extracted (Figure 1(a) and (b)). After healing of extraction sockets for 3 months (Figure 1(c)), alveolar bone defects were created bilaterally. A mid-crestal incision between the second and fourth premolars (PM2, PM4) was made (Figure 1(d)). After full-thickness flaps were raised, four-wall critical-sized alveolar bone defects (4 mm \times 2 mm \times 5 mm, length \times width \times depth) were prepared at the mesial side of PM4 and the distal side of PM2 with 1–2 mm distance between defects and premolars (Figure 1(e)). As described previously, 4 mm \times 2 mm \times 5 mm is the commonly used size for intrabony alveolar defect in dog models, which does not show complete obliteration when left untreated.^{20–23} Four defects were created in each dog.

The four defects in each dog were randomly divided into four groups ($n=6$): (1) negative control group, no treatment; (2) PuraMatrix group, transplantation of PuraMatrix; (3) Vector-cPDLSCs + PuraMatrix group, transplantation of Vector-cPDLSCs/PuraMatrix constructs; and (4) EfnB2-cPDLSCs + PuraMatrix group, transplantation of EfnB2-cPDLSCs/PuraMatrix constructs (Figure 1(f)). All defects were covered by gelatin membranes (Bio-Gide; Geistlich Biomaterials, Wolhusen, Switzerland; Figure 1(g)). To decrease tension, mesial and distal releasing incisions were made. The flaps were then repositioned, and tension-free wound closure was achieved with the use of vertical mattress sutures (Figure 1(h)). Antibiotics (amoxicillin, 15 mg/kg) were administered intramuscularly to each dog for 3 days after surgery. Sutures were removed 7 days later (Figure 1(i)).

Micro-computed tomography analysis

After healing periods of 4 weeks ($n=3$) and 8 weeks ($n=3$), dogs were deeply anesthetized and the oral tissues were fixed by 4% (w/v) paraformaldehyde cardiovascular perfusion. Dogs were then sacrificed by isoflurane inhalation overdose. Blocks containing the defect regions along with adjacent soft and hard tissues were dissected and fixed in 10% buffered formalin for 1 week, and then blocks were scanned and analyzed using a micro-computed tomography (micro-CT) scanner (Scanco Medical AG, Brüttsellen, Zurich, Switzerland) at 80 kV and 116 μ A. Slice thickness was 25 μ m. Images were reconstructed using a three-dimensional structural analysis software (TRI/3D-BON; Ratoc System Engineering, Tokyo, Japan). The region of interest was placed where the original defect was located, as the borders were visually recognizable. Trabecular bone volume per tissue volume (BV/TV), trabecular number (Tb.N), trabecular thickness (Tb.Th), trabecular spacing (Tb.Sp), connectivity density (Conn-Den), and structure model index (SMI) were measured.

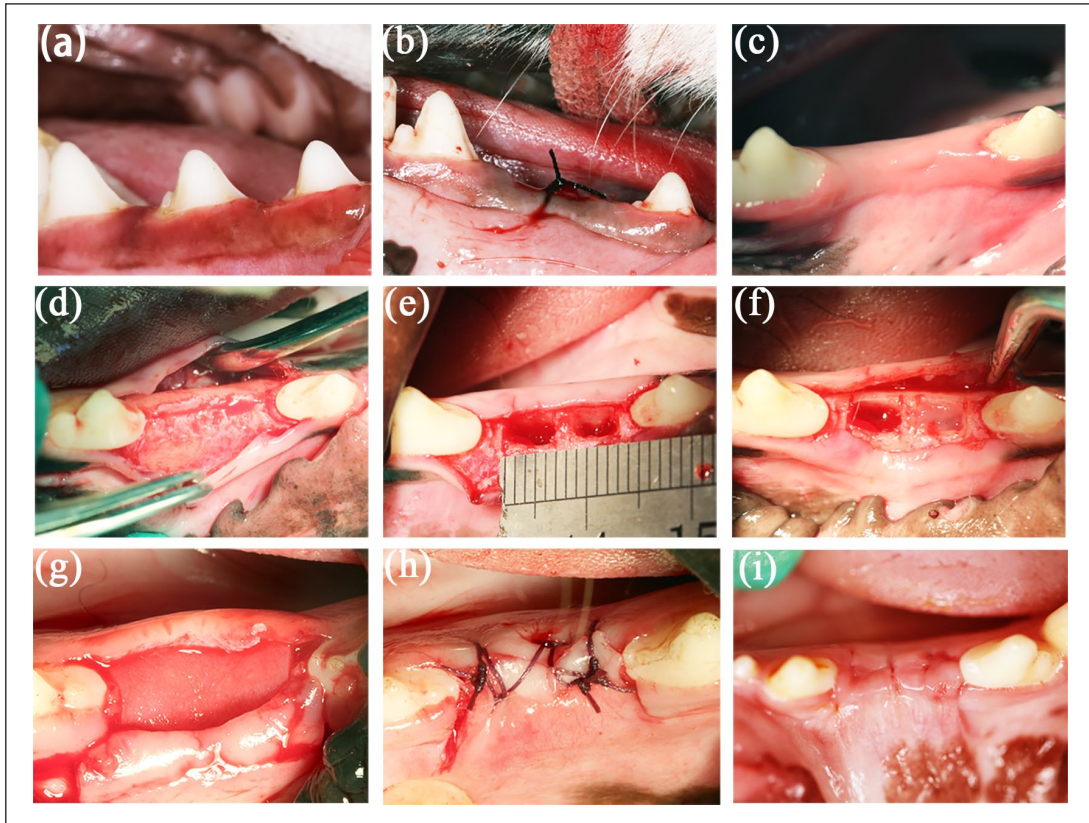


Figure 1. Surgical procedures for animal experiments: (a–d) Bilateral mandibular third premolars were extracted; the extraction sockets healed well after 3 months. (e) Defects (4 mm × 2 mm × 5 mm, length × width × depth) were prepared. (f) Defects were randomly filled with different combinations of cells and PuraMatrix complexes. (g and h) Bio-guide membranes were placed, and tension-free wound closure was achieved. (i) Postoperative view after 1 week.

Statistical analysis

Each experiment was independently conducted three times. Values are shown as mean ± standard deviation (SD). The normal distribution of data and homogeneity of variance were tested first. Depending on the results, first the parametric one-way analysis of variance (ANOVA), followed by the Bonferroni test or the nonparametric Kruskal–Wallis *H*-test and then Dunnett's T3 test was used to compare values among three or more groups. Meanwhile, the parametric Student's *t*-test or the nonparametric Mann–Whitney *U*-test was used to compare two variables. Differences were considered significant when $p < 0.05$.

Results

Characterization of hPDLSCs

We isolated primary hPDLSCs from human third molars (Figure 2(a)) and assessed their colony-forming properties, multiple differentiation potential, and expression of stem cell markers. Colony-forming units were observed with crystal violet staining (Figure 2(b)). Mineralized nodule formation, lipid-rich vacuole formation, and β III-tubulin expression were enhanced after osteogenic, adipogenic, and neurogenic

induction, respectively (Figure 2(c)). The hPDLSCs were positive for CD73, CD90, and CD105 and negative for CD45; 6.08% of the cells were STRO-1 positive (Figure 2(d)).

EphrinB2, phosphorylated ephrinB2, and EphB4 expression was upregulated in hPDLSCs after osteogenic induction

To determine the role of ephrinB2 and its receptor EphB4 in osteogenic differentiation of hPDLSCs, we analyzed the expression of ephrinB2, EphB4, and their phosphorylated forms using Western blotting. EphrinB2 and phosphorylated ephrinB2 (p-ephrinB2) were upregulated in induced hPDLSCs versus non-induced controls on days 3 and 5 (Figure 3(a)–(c)). The expression of EphB4 also increased in induced hPDLSCs versus non-induced controls, while that of phosphorylated EphB4 (p-EphB4) did not increase (Figure 3(a), (d), and (e)).

Overexpression of ephrinB2 stimulated osteogenic differentiation of hPDLSCs

To find out whether ephrinB2 overexpression stimulated osteogenic differentiation of hPDLSCs, we transduced the

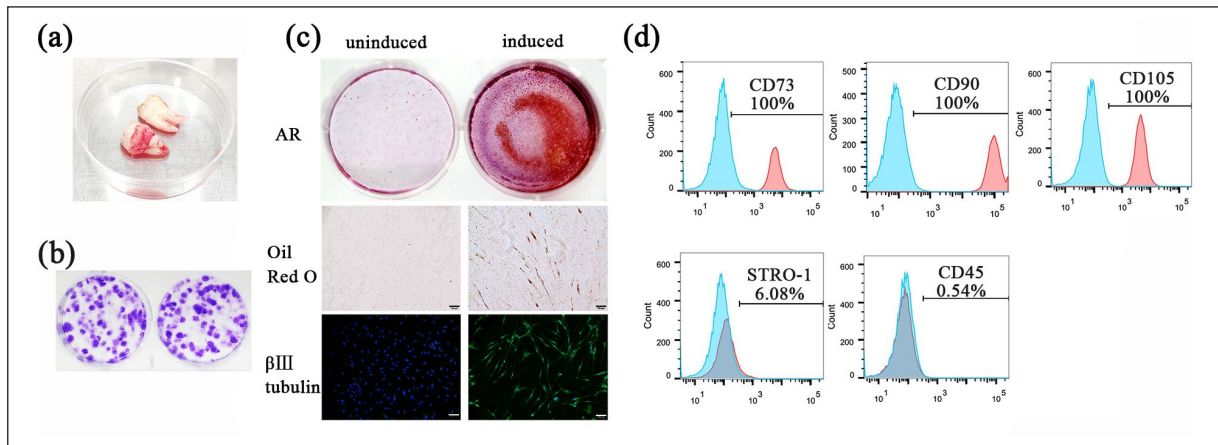


Figure 2. Culture and characterization of hPDLSCs: (a) hPDLSCs were isolated from the middle-third root surfaces of human third molars via enzymatic digestion. (b) Cell colonies were visualized with crystal violet staining. (c) hPDLSCs were cultured in osteogenic, adipogenic, or neurogenic induction medium for 4 weeks; then mineralized nodules, lipid-rich vacuoles, and β III-tubulin expression were assessed. Scale bar: 100 μ m. (d) hPDLSCs were CD73⁺, CD90⁺, CD105⁺, STRO-1⁺, and CD45⁻ when analyzed by flow cytometry. hPDLSCs were at passage 2. Experiments were performed in triplicate.

ephrinB2 gene into hPDLSCs using a lentiviral vector. We observed green fluorescence in ephrinB2-transduced hPDLSCs (EfnB2-hPDLSCs) (Figure 4(a)). The results of qPCR and Western blotting analysis confirmed that ephrinB2 mRNA and protein were upregulated in EfnB2-hPDLSCs (Figure 4(b) and (c)), which proliferated more slowly than Vector-PDLSCs (hPDLSCs transduced by control vectors) and wild-type hPDLSCs. Meanwhile, there was no significant difference in proliferation between Vector-PDLSCs and wild-type hPDLSCs (Figure 4(d)). ALP staining (Figure 5(a)), mineral nodule formation (Figure 5(b)), and mRNA levels of ALP, RUNX2, bone morphogenetic protein 2 (BMP2), and collagen type I (COL1) (Figure 5(c)) were significantly enhanced in EfnB2-hPDLSCs versus Vector-hPDLSCs.

Culture, characterization, and transfection of cPDLSCs

cPDLSCs from canine anterior teeth were isolated and characterized (Figure 6(a)). Colony-forming capacity (Figure 6(b)) and expression of CD73, CD90, CD105, and STRO-1 were confirmed (Figure 6(c)). Osteogenically induced cPDLSCs generated a great number of mineralized nodules and expressed higher levels of ALP (Figure 6(d)). Transcriptions of ALP, BMP2, RUNX2, and COL1 in osteogenically induced cPDLSCs were enhanced on day 21 (Figure 6(e)). In addition, we observed lipid-rich vacuoles and β III-tubulin expression in cPDLSCs after adipogenic and neurogenic induction, respectively (Figure 6(f)). EphB4 and ephrinB2 in osteogenically induced cPDLSCs were upregulated on days 14 and 21, respectively (Figure 6(g)). We confirmed that EfnB2-cPDLSCs expressed green fluorescence (Figure 7(a)) and overexpressed ephrinB2 mRNA

and protein (Figure 7(b)). Alizarin Red S staining and the qPCR assay showed that mineral nodule formation and mRNA levels of RUNX2 and BMP2 were significantly upregulated in EfnB2-cPDLSCs versus Vector-cPDLSCs (Figure 7(c) and (d)).

EphrinB2-modified cPDLSCs promoted alveolar bone regeneration in beagles

To investigate whether ephrinB2-modified cPDLSCs promoted alveolar bone regeneration in vivo, we created an alveolar bone defect model in beagles. After being embedded in PuraMatrix, cPDLSCs exhibited cytoplasmic elongations and grew denser and denser over time, which confirmed their survival in PuraMatrix (Figure 7(e)). We filled the defects with EfnB2-cPDLSCs + PuraMatrix, Vector-cPDLSCs + PuraMatrix, or PuraMatrix alone; completely untreated defects were treated as negative controls.

There was no significant difference in BV/TV, Tb.N, Tb.Th, Tb.Sp, Conn-Den, or SMI between the PuraMatrix and negative control groups, suggesting that PuraMatrix had no significant effect on osteogenesis. BV/TV and Tb.Th of the defects in the EfnB2-cPDLSCs + PuraMatrix group were, respectively, 0.68- and 0.94-fold higher than in the Vector-cPDLSCs + PuraMatrix group. Defects in the EfnB2-cPDLSCs + PuraMatrix group had the lowest SMI, which suggested that this group had a much denser and plate-like trabecular bone (Figure 8(a) and (b)). At 8 weeks, BV/TV in the EfnB2-cPDLSCs + PuraMatrix group was higher than in the other groups. Tb.Th was higher in the EfnB2-cPDLSCs + PuraMatrix group than in the Vector-cPDLSCs + PuraMatrix group. The EfnB2-cPDLSCs + PuraMatrix group had the lowest SMI of all the four groups (Figure 8(a) and (b)).

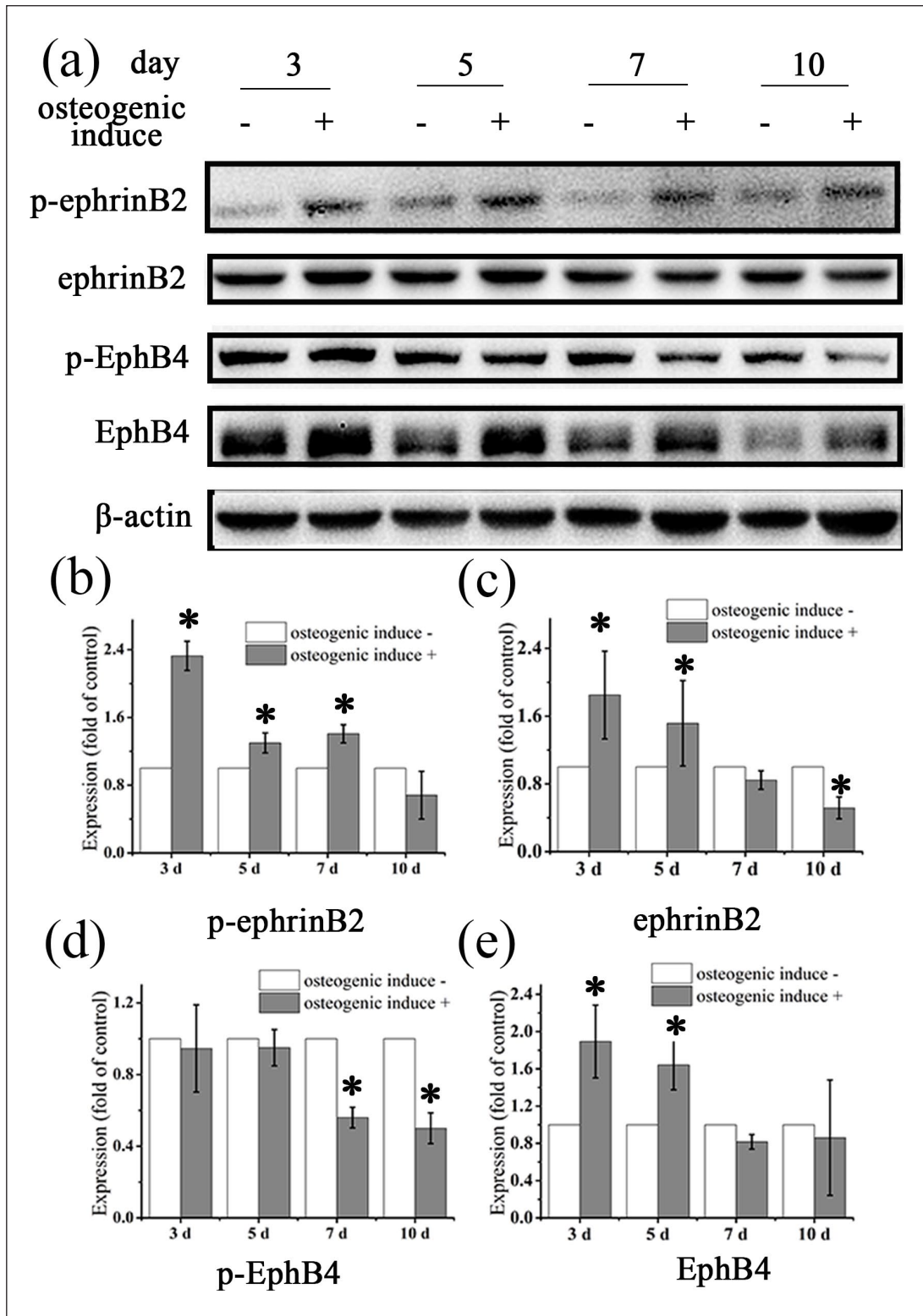


Figure 3. EphrinB2, p-ephrinB2 and EphB4 expression increased in hPDLSCs under osteogenic induction: (a) EphrinB2, EphB4, p-ephrinB2, and p-EphB4 in hPDLSCs were analyzed by Western blotting 3, 5, 7, and 10 days after osteogenic induction. (b–e) Densitometric analysis was performed. The relative level of protein was normalized to β -actin and expressed as fold change over control. (b, c) p-ephrinB2 expression increased on days 3, 5, and 7 after induction, and ephrinB2 expression increased on days 3 and 5. (c, e) EphB4 was upregulated on days 3 and 5 after induction, while p-EphB4 did not increase. These experiments were performed in triplicate. Data are presented as mean \pm SD. * $p < 0.05$ vs control.

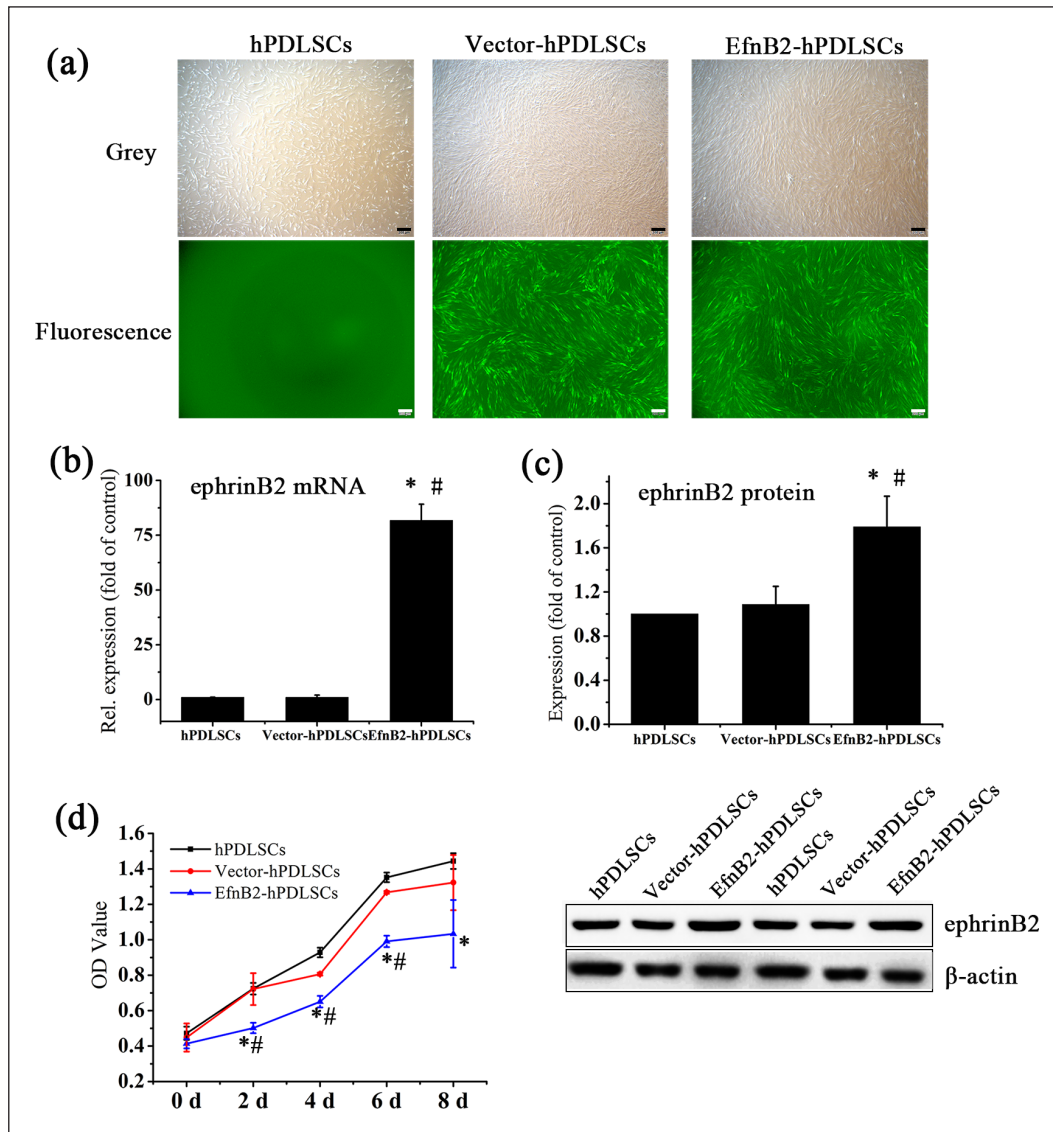


Figure 4. Overexpression of ephrinB2 in hPDLSCs. hPDLSCs were infected with ephrinB2 lentiviral vectors (EfnB2-hPDLSCs) or corresponding control vectors (Vector-hPDLSCs), and wild-type hPDLSCs were used as negative controls. (a) Both EfnB2-hPDLSCs and Vector-hPDLSCs expressed green fluorescence 3 days after infection. Scale bar: 200 μ m. (b, c) Levels of ephrinB2 mRNA and protein in EfnB2-hPDLSCs were higher than those in Vector-hPDLSCs and wild-type hPDLSCs, as confirmed by qPCR and Western blotting analyses. (d) The proliferation rate of EfnB2-hPDLSCs was lower than those of Vector-hPDLSCs and wild-type hPDLSCs. Experiments were performed in triplicate. Data are represented as mean \pm SD. # p < 0.05 vs Vector-hPDLSCs, * p < 0.05 vs wild-type hPDLSCs.

Discussion

Stem cell-based tissue engineering is a promising strategy for regenerating alveolar bone defects. PDLSCs and other osteogenic stem cells, if well tunable, could play critical roles in bone regeneration. It has been reported that ephrinB2/EphB4 signaling regulates osteogenic differentiation of osteoblasts^{11,12,14,17,18,24} and BMSCs.^{12,25,26} Ablation of ephrinB2 expression in osteoblasts was shown to impair osteoblastic differentiation and bone mineralization;²⁷ blocking ephrinB2/EphB4 interaction inhibited osteoblastic differentiation in vitro and in

vivo.¹⁸ Consistent with these findings, in this study we found that under conditions of osteogenic differentiation, ephrinB2 and p-ephrinB2 were significantly elevated in hPDLSCs, confirming the role played by ephrinB2 in regulating hPDLSC osteogenic capacity.

Although ephrinB2 can bind to various EphB receptors, several studies have revealed that ephrinB2/EphB4 interaction in osteoblasts specifically stimulates osteogenic differentiation.^{11,16} Therefore, we analyzed EphB4 and p-EphB4 expression in hPDLSCs under osteogenic induction. However, the level of p-EphB4 did not increase,

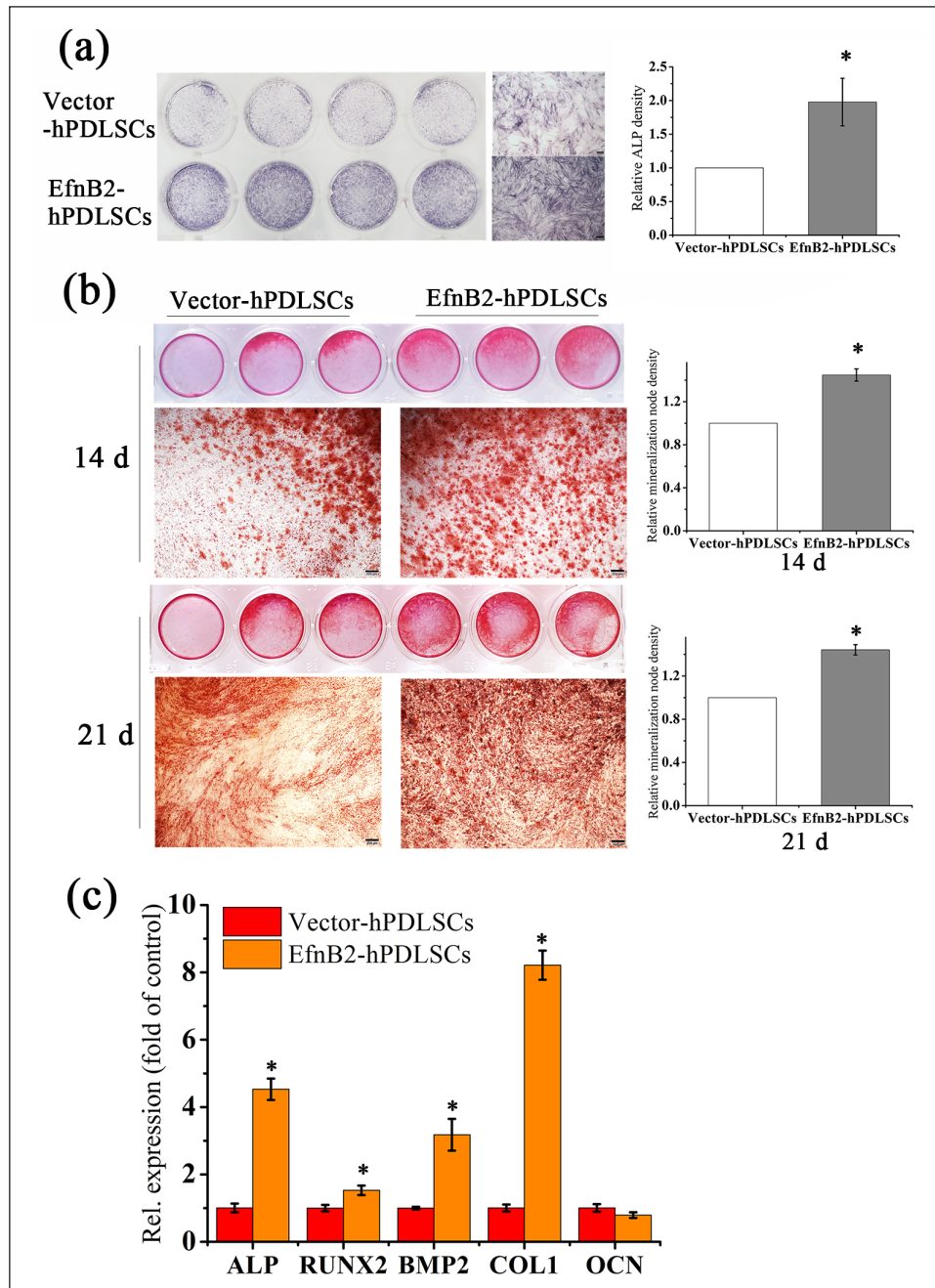


Figure 5. Overexpression of ephrinB2 stimulated osteogenic differentiation of hPDLSCs. To investigate whether overexpression of ephrinB2 contributed to osteogenic differentiation of hPDLSCs, we assessed differences in ALP staining, mineral nodule formation, and osteogenic gene expression between EfnB2-hPDLSCs and Vector-hPDLSCs. (a) ALP staining intensity of EfnB2-hPDLSCs was more profound than that of Vector-hPDLSCs on day 7 after induction, as quantified using Image J software. Scale bar: 200 μ m. (b) Alizarin Red S staining of induced EfnB2-hPDLSCs was stronger than that of Vector-hPDLSCs on days 14 and 21, as quantified using Image J software. Scale bar: 200 μ m. (c) ALP, RUNX2, BMP2, and COL1 transcription was significantly upregulated in EfnB2-hPDLSCs. Experiments were performed in triplicate. Data are represented as mean \pm SD. * $p < 0.05$ vs Vector-hPDLSCs.

suggesting the possibility of other signaling pathways' involvement in hPDLSC osteogenic differentiation. EphB1 and EphB2 are reported to be candidate receptors for ephrinB2 in calvarial bone formation;¹⁴ therefore, it can be assumed that ephrinB2 interacts with EphB1/EphB2 instead of EphB4 in hPDLSCs.

One study reports that ephrinB2 overexpression in BMSCs enhanced osteogenic differentiation of the BMSCs.²⁸ It can therefore be hypothesized that overexpression of ephrinB2 could increase the osteogenic potential of PDLSCs. In this study, we constructed ephrinB2-transduced hPDLSCs and confirmed overexpression of ephrinB2. Similar to a

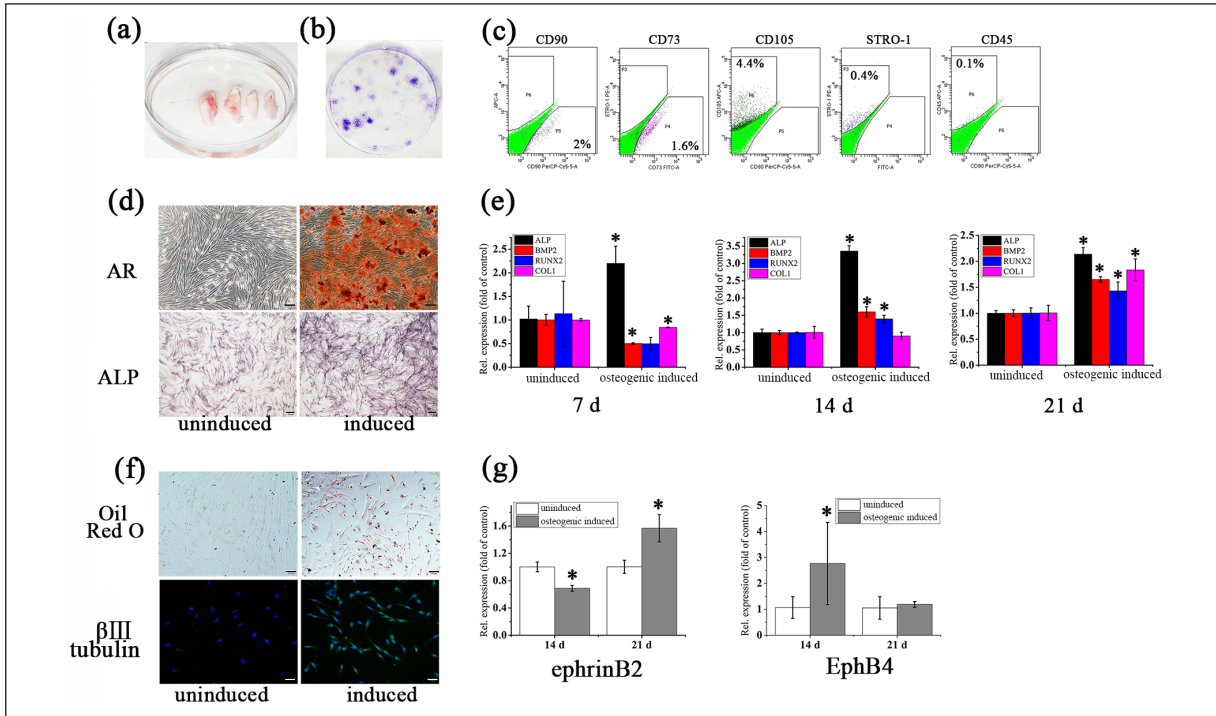


Figure 6. Culture and characterization of cPDLSCs. (a) cPDLSCs were isolated from freshly extracted canine anterior teeth. (b) Colony-formation units were observed after 10 days of culture. (c) Expression of mesenchymal stem cell markers on cPDLSCs was analyzed using flow cytometry. (d) After osteogenic induction, cPDLSCs expressed a greater number of mineralized nodules and higher ALP. Scale bar: upper, 100 μm ; lower, 200 μm . (e) After osteogenic induction, cPDLSCs upregulated ALP transcription on day 7; ALP, BMP2, and RUNX2 transcription on day 14; and ALP, BMP2, RUNX2, and COL1 transcription on day 21. (f) cPDLSCs expressed lipid-rich vacuoles and β III-tubulin after adipogenic and neurogenic induction, respectively, for 4 weeks. Scale bar: upper, 100 μm ; lower, 50 μm . (g) EphB4 and ephrinB2 mRNA increased in osteogenic cPDLSCs on days 14 and 21, respectively. Experiments were performed in triplicate. Data are represented as mean \pm SD. * $p < 0.05$ vs non-induced group.

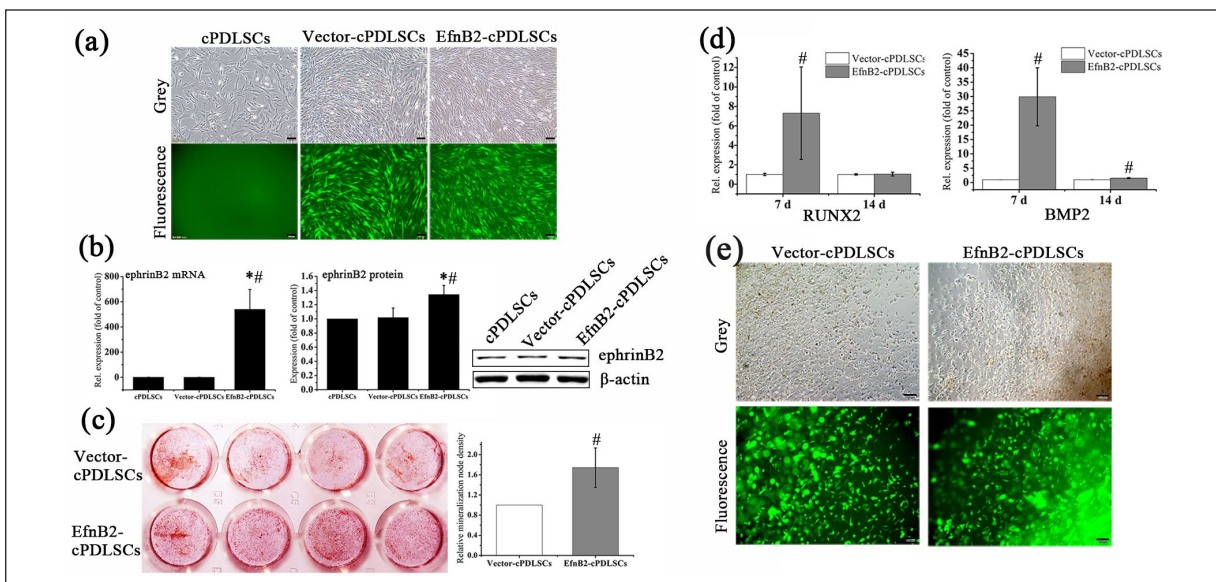


Figure 7. Overexpression of ephrinB2 stimulated osteogenic differentiation of cPDLSCs. (a) Green fluorescence was observed in EfnB2-cPDLSCs on day 3 after infection. Scale bar: 100 μm . (b) EfnB2-cPDLSCs had higher levels of ephrinB2 mRNA and protein than Vector-PDLSCs and wide-type hPDLSCs did. (c) Alizarin Red S staining revealed more mineral nodules in induced EfnB2-cPDLSCs on day 21. (d) RUNX2 and BMP2 were upregulated in EfnB2-cPDLSCs compared with Vector-hPDLSCs. (e) cPDLSCs exhibited cytoplasmic elongations in PuraMatrix. Experiments were performed in triplicate. Scale bar: 100 μm . Data are represented as mean \pm SD. # $p < 0.05$ vs Vector-cPDLSCs, * $p < 0.05$ vs cPDLSCs.

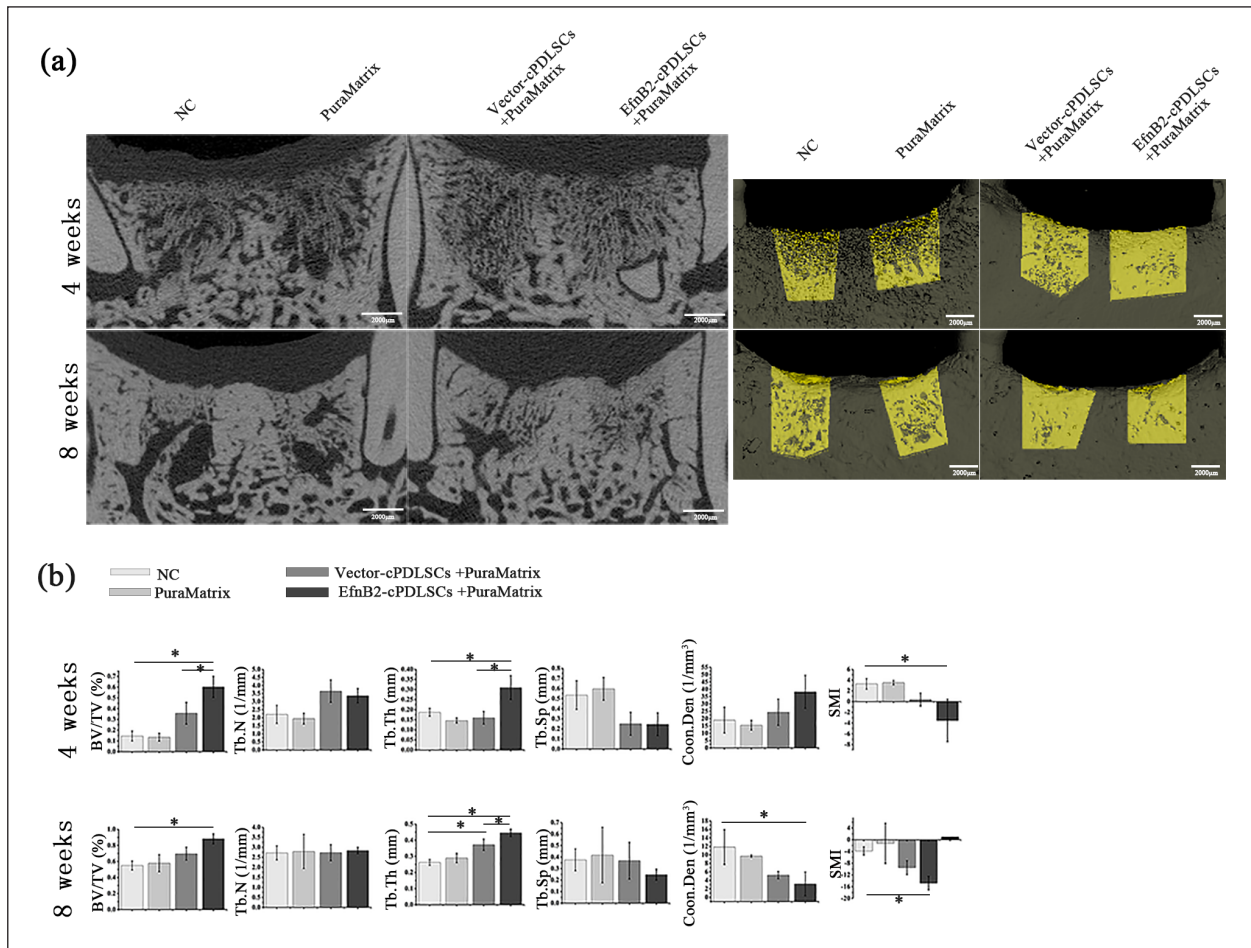


Figure 8. Two-dimensional (2D) and three-dimensional (3D) images of new bone formation by micro-CT and quantitative analysis after 4 and 8 weeks: (a) 2D images of representative sagittal slices and 3D reconstruction of alveolar bone defect regions (newly formed bone shown in yellow). A higher level of new bone formation could be observed in the EfnB2-cPDLSCs group. Scale bar: 2000 μm. (b) New bone volume and various trabecular parameters were compared among the four groups at 4 and 8 weeks. Data are shown as mean ± SD ($n = 3$). * $p < 0.05$. BV/TV: trabecular bone volume per tissue volume; Tb.N: trabecular number; Tb.Th; trabecular thickness; Tb.Sp: trabecular spacing; Conn-Den: connectivity density; SMI: structure model index.

previous study in which BMP2 was transfected into hPDLSCs,²⁹ we saw that EfnB2-hPDLSCs proliferated more slowly than Vector-PDLSCs and wild-type hPDLSCs did. The low proliferation rate of EfnB2-hPDLSCs might have been due to cytotoxicity from lentiviral particles. Compared with Vector-hPDLSCs, EfnB2-hPDLSCs expressed higher levels of ALP, RUNX2, BMP2, and COL1 mRNA, together with deposition of a greater number of calcified nodules, which corroborated that ephrinB2-modified hPDLSCs possessed greater osteogenic potential.

We used beagles to test the effect of ephrinB2-modified PDLSCs on alveolar bone regeneration; cPDLSCs were cultured successfully. Compared with hPDLSCs, cPDLSCs showed relatively low positivity for mesenchymal stem cell markers, as reported previously.^{30,31} Nevertheless, these cells exhibited colony formation and osteogenic, adipogenic, and neurogenic differentiation capacities in this study, as they had in previous studies.^{30,31} Although BMP2,

COL1, and ephrinB2 mRNA in induced cPDLSCs slightly decreased at early stage, their expression increased on day 21. A previous study also reported that ephrinB2 mRNA in osteogenic/odontogenic-induced human dental pulp stem cells did not increase until day 21.³² Furthermore, ephrinB2-modified cPDLSCs showed greater osteogenic potential, as indicated by formation of a greater number of mineral nodules and upregulation of osteogenic genes such as RUNX2 and BMP2.

Direct injection of dissociated cell suspensions shows poor engraftment and persistence due to washing out and low integration of the transplanted cells.³³ The grafting of natural or synthetic biomaterial frameworks seeded with stem cells offers an effective way to overcome such washing out. In addition, a well-designed biomaterial acts not only as a stem cell scaffold but also as a carrier for controlled release of the growth factors that are also critical to driving regeneration.⁶ PuraMatrix is a self-assembling

peptide hydrogel that has been demonstrated to support the survival and differentiation of progenitor cells and mesenchymal stem cells.^{34–36} It can mimic natural extracellular matrix and has effectively delivered different kinds of cells in tissue engineering.^{35,37,38} In this study, cPDLSCs encapsulated in PuraMatrix extended small processes gradually and grew denser and denser with time, indicating that such cells can survive well in PuraMatrix. To exclude the effect of PuraMatrix on alveolar bone regeneration, we transplanted PuraMatrix without cells as control. We found that the effect of PuraMatrix on bone regeneration was insignificant.

The EfnB2-cPDLSCs + PuraMatrix group had the highest BV/TV at 4 and 8 weeks, indicating that this combination resulted in more new bone. Tb.Th was also significantly higher in the EfnB2-cPDLSCs + PuraMatrix group compared with the Vector-cPDLSCs + PuraMatrix and negative control groups, while there was no significant difference in Tb.N among the four groups. These results suggested that EfnB2-PDLSCs enhanced bone formation mainly by increasing trabecular thickness. There are various methods to evaluate new bone formation, such as radiography, micro-CT, and histological examination. Radiography and micro-CT examinations provide both images of new bone and quantitative parameters, and histological examination intuitively shows the morphology and structure of the new bone tissue. Further studies are needed to histologically verify new bone formation and vascularization of the newborn tissues.

EphrinB2-modified PDLSCs promoted bone regeneration partly due to their greater osteogenic differentiation. In vitro studies have revealed that EfnB2-hPDLSCs and EfnB2-cPDLSCs upregulated osteogenic genes and formed a greater number of calcified nodules after osteogenic induction. Furthermore, ephrinB2 has been demonstrated to stimulate osteogenic differentiation of osteoblasts^{11,13,14,17,18,24} and BMSCs^{12,25,26} and to regulate vascular endothelial growth factor (VEGF)-induced angiogenesis.^{39,40} Therefore, overexpressed ephrinB2 in PDLSCs might also act on adjacent osteoblasts, BMSCs, or endothelial cells to induce osteogenesis and vascularization in vivo.

Conclusion

In conclusion, we found that ephrinB2 signaling played an important role in osteogenic differentiation of PDLSCs, and that overexpression of ephrinB2 by gene transfection into PDLSCs enhanced PDLSCs' osteogenic potential and promoted alveolar bone regeneration in vivo.

Acknowledgements

The authors thank Dongsheng Pei and Ankang Hu (Xuzhou Medical University) for helpful advice and assistance.

Availability of data and materials

All data can be obtained in this manuscript.

Declaration of conflicting interests

The author(s) declared no potential conflicts of interest with respect to the research, authorship, and/or publication of this article.

Ethical approval

Isolation of primary hPDLSCs and the beagle experiments were approved by the Ethics Committee of Xuzhou Medical University and the Experimental Animal Ethics Committee of Xuzhou Medical University (No. 20161108).

Funding

The author(s) disclosed receipt of the following financial support for the research, authorship, and/or publication of this article: This study was supported by a grant from the National Nature Science Foundation of China (No. 81700954).

ORCID iD

Changyong Yuan  <https://orcid.org/0000-0002-3795-134X>

References

- Xu XY, Li X, Wang J, et al. Concise review: periodontal tissue regeneration using stem cells: strategies and translational considerations. *Stem Cells Transl Med* 2019; 8(4): 392–403.
- Onizuka S and Iwata T. Application of periodontal ligament-derived multipotent mesenchymal stromal cell sheets for periodontal regeneration. *Int J Mol Sci* 2019; 20(11): E2796.
- Dan H, Vaquette C, Fisher AG, et al. The influence of cellular source on periodontal regeneration using calcium phosphate coated polycaprolactone scaffold supported cell sheets. *Biomaterials* 2014; 35(1): 113–122.
- Bright R, Hynes K, Gronthos S, et al. Periodontal ligament-derived cells for periodontal regeneration in animal models: a systematic review. *J Periodontol Res* 2015; 50(2): 160–172.
- Izumi Y, Aoki A, Yamada Y, et al. Current and future periodontal tissue engineering. *Periodontol* 2000 2011; 56: 166–187.
- Chen FM, Sun HH, Lu H, et al. Stem cell-delivery therapeutics for periodontal tissue regeneration. *Biomaterials* 2012; 33(27): 6320–6344.
- Menicanin D, Mrozik KM, Wada N, et al. Periodontal-ligament-derived stem cells exhibit the capacity for long-term survival, self-renewal, and egeration of multiple tissue types in vivo. *Stem Cells Dev* 2014; 23: 1001–1011.
- Mrozik KM, Wada N, Marino V, et al. Regeneration of periodontal tissues using allogeneic periodontal ligament stem cells in an ovine model. *Regen Med* 2013; 8(6): 711–723.
- Han J, Menicanin D, Marino V, et al. Assessment of the regenerative potential of allogeneic periodontal ligament stem cells in a rodent periodontal defect model. *J Periodontol Res* 2014; 49(3): 333–345.

10. Iwata T, Yamato M, Tsuchioka H, et al. Periodontal regeneration with multi-layered periodontal ligament-derived cell sheets in a canine model. *Biomaterials* 2009; 30(14): 2716–2723.
11. Zhao C, Irie N, Takada Y, et al. Bidirectional ephrinB2-EphB4 signaling controls bone homeostasis. *Cell Metab* 2006; 4(2): 111–121.
12. Toda H, Yamamoto M, Uyama H, et al. Effect of hydrogel elasticity and ephrinB2-immobilized manner on Runx2 expression of human mesenchymal stem cells. *Acta Biomater* 2017; 58: 312–322.
13. Li C, Shi C, Kim J, et al. Erythropoietin promotes bone formation through EphrinB2/EphB4 signaling. *J Dent Res* 2015; 94(3): 455–463.
14. Benson MD, Opperman LA, Westerlund J, et al. Ephrin-B stimulation of calvarial bone formation. *Dev Dyn* 2012; 241(12): 1901–1910.
15. Hou J, Chen Y, Meng X, et al. Compressive force regulates ephrinB2 and EphB4 in osteoblasts and osteoclasts contributing to alveolar bone resorption during experimental tooth movement. *Korean J Orthod* 2014; 44(6): 320–329.
16. Diercke K, Kohl A, Lux CJ, et al. Strain-dependent up-regulation of ephrin-B2 protein in periodontal ligament fibroblasts contributes to osteogenesis during tooth movement. *J Biol Chem* 2011; 286(43): 37651–37664.
17. Allan EH, Hausler KD, Wei T, et al. EphrinB2 regulation by PTH and PTHrP revealed by molecular profiling in differentiating osteoblasts. *J Bone Miner Res* 2008; 23(8): 1170–1181.
18. Takyar FM, Tonna S, Ho PW, et al. EphrinB2/EphB4 inhibition in the osteoblast lineage modifies the anabolic response to parathyroid hormone. *J Bone Miner Res* 2013; 28(4): 912–925.
19. Li M, Zhang C, Jin L, et al. Porphyromonas gingivalis lipopolysaccharide regulates ephrin/Eph signalling in human periodontal ligament fibroblasts. *J Periodontal Res* 2017; 52(5): 913–921.
20. Marei HF, Mahmood K and Almas K. Critical size defects for bone regeneration experiments in the dog mandible: a systematic review. *Implant Dent* 2018; 27(1): 135–141.
21. Zang SQ, Kang S, Hu X, et al. Comparison of different periodontal healing of critical size noncontained and contained intrabony defects in beagles. *Chin Med J* 2017; 130(4): 477–486.
22. Nunez J, Sanz-Blasco S, Vignoletti F, et al. Periodontal regeneration following implantation of cementum and periodontal ligament-derived cells. *J Periodontal Res* 2012; 47(1): 33–44.
23. Nagayasu-Tanaka T, Anzai J, Takaki S, et al. Action Mechanism of Fibroblast Growth Factor-2 (FGF-2) in the promotion of periodontal regeneration in beagle dogs. *PLoS ONE* 2015; 10(6): e0131870.
24. Martin TJ, Allan EH, Ho PW, et al. Communication between ephrinB2 and EphB4 within the osteoblast lineage. *Adv Exp Med Biol* 2010; 658: 51–60.
25. Zhang F, Zhang Z, Sun D, et al. EphB4 promotes osteogenesis of CTLA4-modified bone marrow-derived mesenchymal stem cells through cross talk with Wnt pathway in xenotransplantation. *Tissue Eng Part A* 2015; 21(17–18): 2404–2416.
26. De Luca I, Di Salle A, Alessio N, et al. Positively charged polymers modulate the fate of human mesenchymal stromal cells via ephrinB2/EphB4 signaling. *Stem Cell Res* 2016; 17(2): 248–255.
27. Tonna S, Takyar FM, Vrahnas C, et al. EphrinB2 signaling in osteoblasts promotes bone mineralization by preventing apoptosis. *FASEB J* 2014; 28(10): 4482–4496.
28. Tierney EG, McSorley K, Hastings CL, et al. High levels of ephrinB2 over-expression increases the osteogenic differentiation of human mesenchymal stem cells and promotes enhanced cell mediated mineralisation in a polyethyleneimine-ephrinB2 gene-activated matrix. *J Control Release* 2013; 165(3): 173–182.
29. Jung IH, Lee SH, Jun CM, et al. Characterization of the enhanced bone regenerative capacity of human periodontal ligament stem cells engineered to express the gene encoding bone morphogenetic protein 2. *Tissue Eng Part A* 2014; 20(15–16): 2189–2199.
30. Dissanayaka WL, Zhu X, Zhang C, et al. Characterization of dental pulp stem cells isolated from canine premolars. *J Endod* 2011; 37(8): 1074–1080.
31. Wang WJ, Zhao YM, Lin BC, et al. Identification of multipotent stem cells from adult dog periodontal ligament. *Eur J Oral Sci* 2012; 120(4): 303–310.
32. Heng BC, Wang S, Gong T, et al. EphrinB2 signaling enhances osteogenic/odontogenic differentiation of human dental pulp stem cells. *Arch Oral Biol* 2018; 87: 62–71.
33. Haraguchi Y, Shimizu T, Sasagawa T, et al. Fabrication of functional three-dimensional tissues by stacking cell sheets in vitro. *Nat Protoc* 2012; 7(5): 850–858.
34. Cavalcanti BN, Zeitlin BD and Nor JE. A hydrogel scaffold that maintains viability and supports differentiation of dental pulp stem cells. *Dent Mater* 2013; 29(1): 97–102.
35. Wu G, Pan M, Wang X, et al. Osteogenesis of peripheral blood mesenchymal stem cells in self assembling peptide nanofiber for healing critical size calvarial bony defect. *Sci Rep* 2015; 5: 16681.
36. Ortinau S, Schmich J, Block S, et al. Effect of 3D-scaffold formation on differentiation and survival in human neural progenitor cells. *Biomed Eng Online* 2010; 9: 70.
37. Dissanayaka WL, Hargreaves KM, Jin L, et al. The interplay of dental pulp stem cells and endothelial cells in an injectable peptide hydrogel on angiogenesis and pulp regeneration in vivo. *Tissue Eng Part A* 2015; 21(3–4): 550–563.
38. Tcacencu I, Karlstrom E, Cedervall J, et al. Transplanted human bone marrow mesenchymal stem cells seeded onto peptide hydrogel decrease alveolar bone loss. *Biores Open Access* 2012; 1(5): 215–221.
39. Sawamiphak S, Seidel S, Essmann CL, et al. Ephrin-B2 regulates VEGFR2 function in developmental and tumour angiogenesis. *Nature* 2010; 465(7297): 487–491.
40. Wang Y, Nakayama M, Pitulescu ME, et al. Ephrin-B2 controls VEGF-induced angiogenesis and lymphangiogenesis. *Nature* 2010; 465(7297): 483–486.